Leukemia Research 37 (2013) 1374–1382

Contents lists available at ScienceDirect

Leukemia Research

journal homepage: www.elsevier.com/locate/leukres

Live cell detection of chromosome 2 deletion and Sfpi1/PU1 loss in radiation-induced mouse acute myeloid leukaemia

C.-H. Olme, R. Finnon, N. Brown, S. Kabacik, S.D. Bouffler, C. Badie*

Biological Effects Department, Centre for Radiation, Chemical and Environmental Hazards, Public Health England, Chilton, Didcot, Oxfordshire, UK

ARTICLE INFO

Article history:
Received 21 February 2013
Received in revised form 24 May 2013
Accepted 26 May 2013
Available online 25 June 2013

Keywords:
Radiation
Live cells
Chromosome deletion
Sfpi1/PU.1
Myeloid leukaemia
Mouse model

ABSTRACT

The CBA/H mouse model of radiation-induced acute myeloid leukaemia (rAML) has been studied for decades to bring to light the molecular mechanisms associated with multistage carcinogenesis. A specific interstitial deletion of chromosome 2 found in a high proportion of rAML is recognised as the initiating event. The deletion leads to the loss of *Sfpi*, a gene essential for haematopoietic development. Its product, the transcription factor PU.1 acts as a tumour suppressor in this model. Although the deletion can be detected early following ionising radiation exposure by cytogenetic techniques, precise characterisation of the haematopoietic cells carrying the deletion and the study of their fate *in vivo* cannot be achieved. Here, using a genetically engineered C57BL/6 mouse model expressing the GFP fluorescent molecule under the control of the *Sfpi1* promoter, which we have bred onto the rAML-susceptible CBA/H strain, we demonstrate that GFP expression did not interfere with X-ray induced leukaemia incidence and that GFP fluorescence in live leukaemic cells is a surrogate marker of radiation-induced chromosome 2 deletions with or without point mutations on the remaining allele of the *Sfpi1* gene. This study presents the first experimental evidence for the detection of this leukaemia initiating event in live leukemic cells.

1. Background

Ionising radiation (IR) is a well known carcinogen in humans. Epidemiological studies of mortality and incidence of cancer have shown an increased risk of cancer in the Japanese atomic bomb survivors, in those exposed to ionising radiation therapeutically and in the nuclear industry workers [1–4]. In survivors of the Hiroshima and Nagasaki atomic bombs, an excess risk in solid cancers was found and an approximately 5-fold increase in leukaemias, including acute lymphocytic leukaemia, chronic myeloid leukaemia and AML was seen [5]. However, formal identification of human cancers known to be caused specifically by radiation exposure remains an unsolved issue and there is no comprehensive understanding of the molecular mechanisms of cancer induction by IR.

Animal models of human cancers are extremely valuable for a better understanding of the molecular mechanisms of tumour initiation and development, in particular for cancers induced by environmental agents such as IR. rAML is one IR induced tumour for which mouse models are available. The CBA model of rAML, has been used for over 30 years to study rAML [6]. It is a particularly valuable model due to the very low spontaneous AML incidence [7]. A single whole-body exposure of X-rays at a dose of 3 gray gave maximal yields around 25% [6]. In the mice that develop rAML, it has been found that over 90% of the leukaemic blasts have a partial deletion of one copy of chromosome 2 in CBA/H mice and other strains susceptible to the disease [7–11]. Chromosome 2 interstitial deletions (Del2) are characteristic of rAML [12]. Cells carrying the chromosome deletion start to expand clonally in 50% of the animals around 12 months after radiation exposure, probably due to a proliferative or selective advantage, but ultimately up to only 25% of the mice are diagnosed with rAML suggesting that other molecular events arising spontaneously are required for AML development [6,13]. Del2 can be seen in bone marrow from all CBA/H mice irradiated with a whole-body dose of 3 Gy 24 h after exposure and although this early chromosome deletion does not lead directly to rAML in all mice, this event is considered the initiating molecular event that potentially leads to leukaemia [13,14]. The key gene identified in the deleted region is *Sfpi1* coding for the haematopoietic transcription factor PU.1 [15–18]. *Sfpi1* suffers from point mutation in exon 5, the DNA binding domain, following hemizygous loss in approximately 70% rAMLs [11,15,16]. Transcriptional expression levels of *Sfpi1* and PU.1 protein expression, have

* Corresponding author at: Cancer Genetics and Cytogenetics Group, Biological Effects Department, Public Health England, Centre for Radiation, Chemical and Environmental Hazards, Chilton, Didcot, Oxfordshire, UK. Tel.: +44 1235825088; fax: +44 1235833891.
E-mail addresses: Christophe.badie@phe.gov.uk, chris_badie@yahoo.fr (C. Badie).

0145-2126
http://dx.doi.org/10.1016/j.leukres.2013.05.019

been shown in several cases to be important for the maturation and differentiation of haematopoietic cells [19,20]. Importantly, reduction to about 20% of normal levels of the gene or conditional complete inactivation *in vivo* were found to lead to the development of AML [21,22]. Some cases of rAML do not have *Sfpi1* deletions or point mutations and recently we have reported internal tandem duplications in *Flt3* (the most common mutation in human AML) within a panel of rAMLs [23]. An inverse relationship between the expression of the gene *Flt3* and *Sfpi1* has also been observed [24,25].

Currently, Del2 are detected using PCR based loss of heterozygosity in F1 hybrid mice and fluorescence *in situ* hybridisation (FISH) techniques [14,26,27]. However, these are respectively performed on DNA extracts and fixed cells limiting further characterisation. Fundamental questions on the biology of this deletion remain unresolved because of the difficulty in detecting individual Del2-bearing cells *in vivo*. Transgenic mouse models expressing green fluorescent protein (GFP) as a reporter gene for *Sfpi1* expression have been created by two separate research groups to make possible the monitoring of *Sfpi1* expression during hematopoiesis and the development of subpopulations of bone marrow cells [28,29]. Here, we made use of Nutt et al. engineered mouse model by transferring it onto the CBA/H genetic background, postulating that it would be possible to use the GFP expression marker to identify radiation-induced Del2 *ex vivo*. This study presents the first experimental evidence for the detection of copy loss of *Sfpi1* and PU.1 expression in live leukaemic cells.

2. Methods

2.1. Mice

C57BL/6 GFP expressing mice from Steven Nutt were re-derived and backcrossed to a CBA/H background at MRC for at least 10 generations for all experiments (Harwell, Oxon, UK) [28,30]. The GFP construct is situated in the 3′ untranslated region of the *Sfpi1* gene, located on mouse chromosome 2 where GFP is under the control of the Sfpi1 promoter. During transcription a bicistronic mRNA is produced, generating wild-type PU.1 protein and GFP.

Both CBA/H $Sfpi1^{GFP/GFP}$ and CBA/H $Sfpi1^{GFP/+}$ animals (generated from a homozygous male and wild type CBA/H female) were utilised in this study. All animals were bred and handled according to UK Home Office Animals (Scientific Procedures) Act 1986 and with guidance from the local ethical review committee on animal experiments. Details of the original construct, its localisation on mouse chromosome 2 and position of primers used for genotyping are presented in Fig. 1.

2.2. rAML induction experiment

50 male $Sfpi1^{GFP/+}$, 50 male $Sfpi1^{GFP/GFP}$ and 15 female $Sfpi1^{GFP/GFP}$ mice were whole-body 3 Gy irradiated at 12–15 weeks of age with 250 kVp X-rays at a dose rate of 0.887 Gy/min (MRC Radiation and Genome Stability Unit, Harwell, Oxon, UK). AMLs were diagnosed using the criteria described in the Bethesda Proposals for Classification of Non-Lymphoid Neoplasms in mice [31]. Mice were examined daily for signs of illness and euthanised with a rising concentration of CO_2. Animals found to have increased white blood cell counts in the peripheral blood film and displaying splenomegaly or hepatosplenomegaly upon dissection were treated as potential AMLs. Samples of spleen were either stored at −70 °C in RNAlater (Ambion, Austin, US) for nucleic acid extraction or disaggregated and used for FACS or chromosome preparations for cytogenetics. All cases defined as AML had a rapid onset, with ≥20% immature forms/blasts found when spleen cell samples were analysed by flow cytometry, and a white blood cell count above that of controls (controls: approx. $5–10 \times 10^6$/mL). Flow cytometry analysis (as performed below) furthermore established that cases of AML are further defined by the surface marker expression as described in the text.

2.3. Flow cytometry phenotyping of rAML cases

1×10^5 cells were incubated with Fc Block (BD Bioscience), aside from samples stained with antibodies against FcγRIII/II. After transfer to a fresh tube, the following primary antibodies were added (all diluted in PBS/3% BSA), according to manufacturer's recommendations: Gr-1/Ly6G-PE (clone 1A8), CD31-PE, CD3-PE, Flt3-PE (BD Bioscience), Mac-1-PE/Cy5, Ly6C-PE, c-kit-PE, B220 (CD45R)-PE/Cy5, CD34-PE, CD38-PE, VCAM1-PE, Thy-1-PE, FcγRIII/II-PE (Abcam, Cambridge), c-kit-PE/Cy5 and Sca-1-PE (Biolegend, CA USA). Samples were analysed on a FACS Calibur (BD Bioscience) flow cytometer using CellQuest software. Regions were drawn around major populations of cells on a FSC/SSC dot plot. Events with low FSC/SSC were assumed to be dead cells and debris, and excluded from analysis [32]. Analysis was performed on cells with high FSC/SSC. The GFP geometric mean fluorescence intensity (geo MFI) of samples was determined by the mean channel number on a log scale *x*-axis on a histogram or on the lower right quadrant on a dot plot. In experiments where indicated in the text, 7-Aminoactinomycin D (7-AAD) (Sigma) was added, 5 μl/sample.

2.4. PCR and qPCR

To determine *Sfpi1*/GFP construct copy number in rAML and control spleen cells and ear-clip DNA for genotyping, duplex PCR using the following genotyping primers (Sigma) were used:

Forward A-5′ TGGCGCCTACCGGTGGATGTGG 3′
Reverse B-5′ CTGTGTGCCACCACCTGCCTACATT 3′
Forward C-5′ GTGCTTCTTTGGGAGTCTGGCGCT 3′

Primer A and B identifies the 512 base pair (bp) *Sfpi1*/GFP allele and primer B and C identifies the 680 bp wild type *Sfpi1* allele.

To determine the amount of contaminating normal DNA that could be tolerated in the copy number anaylsis of rAMLs, standard mixes of normal splenocyte to leukaemic DNA were used (9:1, 7:3, 1:1, 3:7, 1:9) [33].

Samples (25 ng/μl) were run on a Hybaid PCR express thermocycler (4 min at 95 °C, 45 cycles of 15 s each at 95 °C, 55 °C and 72 °C, and a 10 min at 72 °C). Products were analysed using a 2% agarose gel (BioRad, Hercules, US), stained with ethidium bromide and visualised using UV on a BioRad Gel Doc 2000 system.

For qPCR, reactions were performed as previously described [34,35]. Primer and probe sets used (Eurogentec Ltd., Fawley, Hampshire, UK) are as follows:

***Sfpi1* (forward)** 5′ AGAAGCTGATGGCTTGGAGC 3′
***Sfpi1* (reverse)** 5′ GCGAATCTTTTTCTTGCTGCC 3′
6-Hexachlorofluorescein 5′ TGGGCCAGGTCTTCTGCACGG 3′
***GFP* (forward)** 5′ AGCCGCTACCCCGACCACAT 3′
***GFP* (reverse)** 5′ CGGTTCACCAGGGTGTCGCC 3′
Texas Red 5′ GCCCGAAGGCTACGTCCAGGAGCGC 3′
HPRT (forward) 5′ GGACAGGACTGAAAGACTTG 3′
HPRT (reverse) 5′ TAATCCAGCAGGTCAGCAAA 3′
6-Carboxyfluorescein 5′ CCCTTGAGCACACAGAGGGCCACA 3′.

Gene target cycle threshold (Ct) values were normalised to a hypoxanthine guanine phosphoribosyl transferase (*Hprt*) internal control and were converted to transcript quantity (SQ) using standard curves run with each qPCR plate.

2.5. DNA sequencing and analysis of point mutations

Exon 5 mutations in *Sfpi*1 were determined by DNA sequencing as described [16,25] using primer sequences: F-5′CGACATGAAGGACAGCATCT3′ and R-5′TTTCTTCACCTCGCCTGTCT3′ (Sigma).

2.6. Fluorescent in situ hybridisation (FISH)

2.6.1. Chromosome preparations

Disaggregated spleen cells were cultured at a concentration of $1.5–2 \times 10^6$ cells/mL in 5 mL IMDM/20% FBS, 100 U/mL Penicillin and 100 μg/mL Streptomycin (Fisher Scientific) with addition of 25 μg/mL lipopolysaccharide (Sigma) and 4 μg/mL ConcavalinA (Amersham Biosciences, UK) for 48 h. Colcemid was added at 0.6 μg/mL and incubated for 1 h. After a 15 min hypotonic treatment (0.075 M KCl at 37 °C), cells were fixed (1:3 acetic acid/methanol) and stored at −20 °C until slide preparations.

2.6.2. Bacterial artificial chromosome (BAC) probes and FISH

BAC probes and the FISH technique was carried out on fixed splenocytes using the protocol described [14].

2.7. Statistical analysis

Where statistical analysis has been performed, this was done by a 1-tailed, unpaired Student's *t*-test using Microsoft Excel.

3. Results

3.1. Effect of GFP reporter gene on susceptibility of mice to radiation-induced AML

In order to evaluate whether the GFP cassette would affect the incidence of rAML a total of 115 mice, 50 male *Sfpi1*/GFP heterozygous ($Sfpi1^{GFP/+}$), 50 *Sfpi1*/GFP homozygous ($Sfpi1^{GFP/GFP}$) and

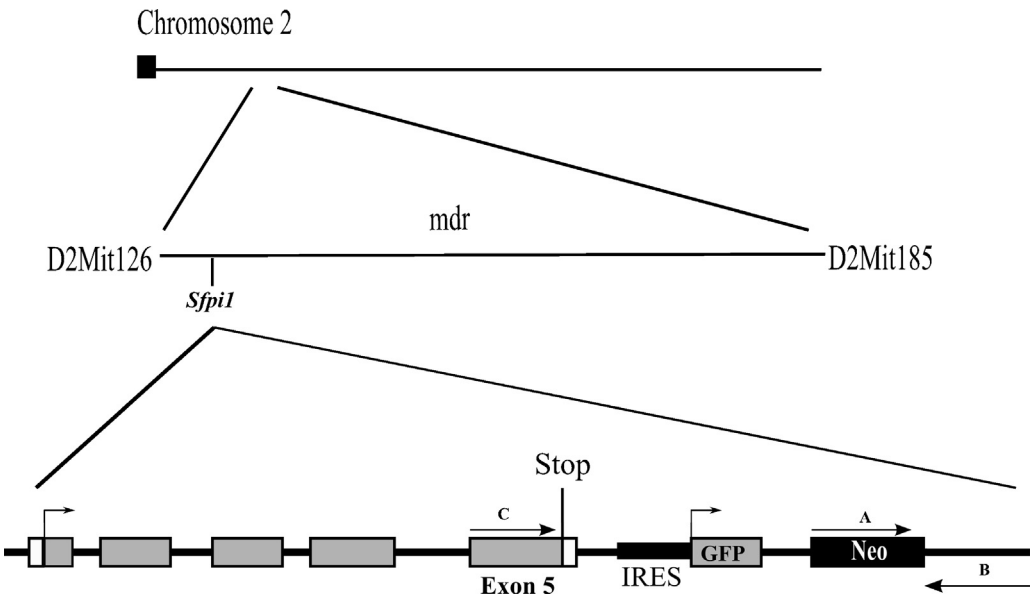

Fig. 1. Location of the GFP construct and a detailed view of the some of its features. The GFP construct is situated in the 3′ untranslated region of the *Sfpi1* gene, located on mouse chromosome 2. The *Sfpi1* gene is located in the AML minimal deleted region (mdr) between D2Mit126 and D2Mit185. Exons of the gene are denoted as boxes with the coding region in grey and introns as a black line, where exon 5 is specifically denoted. The direction of transcription is marked by arrows. Three primer binding sites forward A, reverse B and forward C are indicated. Stop: Stop codon, IRES: internal ribosome entry site, Neo: neomycin cassette.

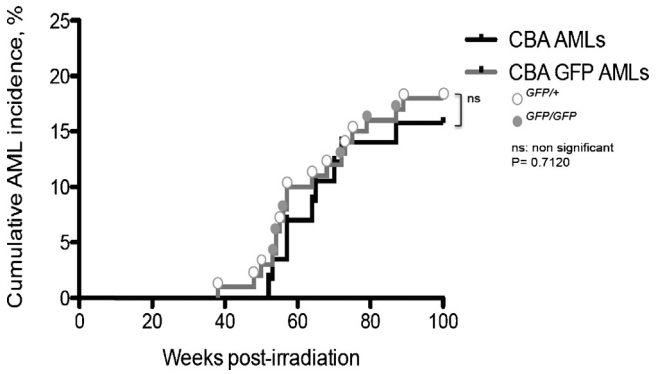

Fig. 2. Leukaemia incidence. Kaplan–Meier analysis of cumulative probability of radiation-induced acute myeloid leukaemia in male CBA/H (total number irradiated = 57, AML induced = 9) and CBA GFP mice (total number irradiated = 100, AML induced = 18) following 3 gray acute whole body X-irradiation. For GFP AMLs, $Sfpi1^{GFP/+}$ individual AMLs are represented by a white circle and $Sfpi1^{GFP/GFP}$ by a grey circle. No significant difference in rAML latency or penetrance was found between CBA and CBA GFP AMLs (log rank $p = 0.712$).

a further 15 $Sfpi1^{GFP/GFP}$ female mice were irradiated with 3 Gy X-rays at 12–15 weeks of age. Previous AML induction experiments within our laboratory (data unpublished) and at other institutions in the last 5 years have seen AML incidences of approximately 16% in male CBA mice. Here we report a similar incidence of 18% in male $Sfpi1^{GFP}$ (*i.e.* $Sfpi1^{GFP/+}$ and $Sfpi1^{GFP/GFP}$) mice, all of which arose in the same window of time; 38–89 weeks (Fig. 2). Only one female (about 7%) out of 15 was diagnosed with AML and this is consistent with previous work describing a lower incidence in CBA/H [36,37].

3.2. Analysis of GFP expression levels in mice by flow cytometry

GFP expression in bone marrow cells from $Sfpi1^{GFP/+}$ and homozygote $Sfpi1^{GFP/GFP}$ mice was analysed by flow cytometry. Control non-GFP mice were used to estimate the level of autofluorescence with apoptotic 7-AAD positive cells being excluded (Fig. 3A). The expression of GFP can be divided into three levels based on the three discrete populations of fluorescence intensity: GFP negative/low, GFP medium and GFP high (Fig. 3B). The percentage of GFP expressing cells in bone marrow is similar between the $Sfpi1^{GFP/+}$ and $Sfpi1^{GFP/GFP}$ mice in each level, 15% and 17% (GFP low), and 26% and 31% (GFP high). Overlaying histograms for $Sfpi1^{GFP/+}$ and $Sfpi1^{GFP/GFP}$ mice shows that GFP expression in heterozygotes is close to 50% of that in homozygote mice.

Examination of RNA levels of *Sfpi1* and GFP by quantitative polymerase chain reaction (qPCR) showed a good correlation between the levels of GFP mRNA and the copy number of the construct (Fig. 3C) with $Sfpi1^{GFP/GFP}$ mice having around double the amount of GFP mRNA compared to $Sfpi1^{GFP/+}$ mice (mean 1.0 and 0.54 respectively, $p = 0.000004$) thus confirming that GFP expression is a sensitive surrogate of *Sfpi1* expression.

3.3. Phenotyping of rAML cases using flow cytometry

Immunophenotyping was carried out on all suspected rAML cases using an antibody panel based on published recommendations [31,38]. The major populations of cells were gated on a forward scatter (FSC)/side scatter (SSC) dot plot. GFP expression was analysed on an unstained sample and the percentage positive cells obtained from percentage events in the GFP single positive quadrant of a dot plot. The geometric mean fluorescence intensity was determined from the same quadrant. Percentage positive cells for a specific surface marker were obtained by combining the percentage of the two upper quadrants in the dot plot.

All rAML cases are negative for the two lymphoid markers CD3 and B220 and for CD38, apart from 57.3b (Supplementary Table 1), which we believe has a mixed-lineage leukaemia phenotype. Furthermore the phenotype was CD34 negative, positive for myeloid markers Mac-1, FcγRIII/II, CD31 and Ly6C, and positive for the stem cell marker c-Kit with a variable expression of Gr-1, Sca-1, Flt3, VCAM-1 and Thy-1 (Fig. 4B and Supplementary Table 1). This suggests an immunophenotype of acute monocytic leukaemias with a variable granulocytic component, and a single bi-phenotypic case. The detailed surface marker expression of a panel of 9 samples can be seen in supplementary Table 1. Differential cell counts, neutropenia and blast cell morphology in blood films confirm this diagnosis of a monocytic lineage.

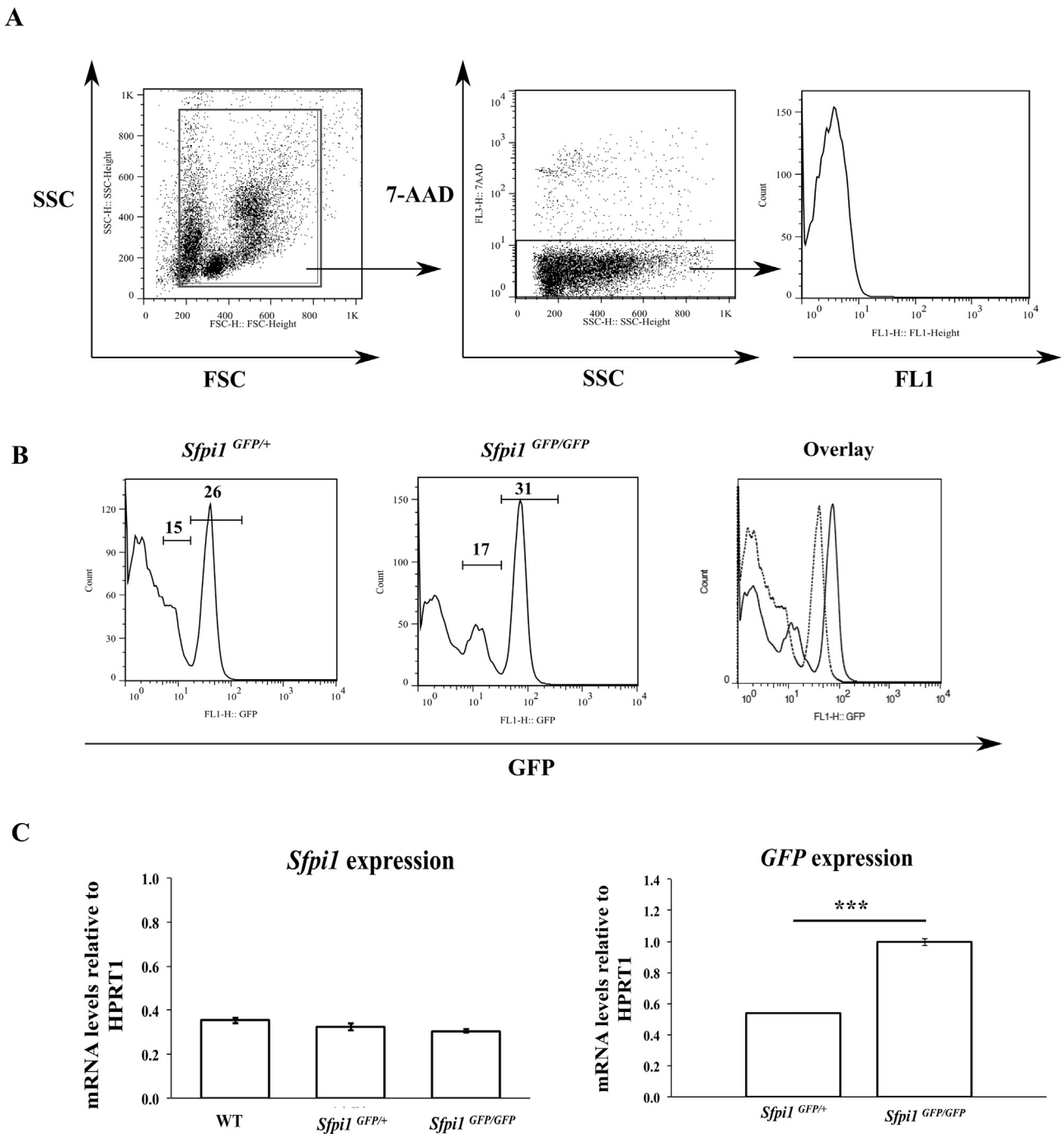

Fig. 3. The correlation between GFP expression and *Sfpi1* expression. (A) Bone marrow cells were extracted from femora and tibias, washed in PBS and analysed by flow cytometry with the addition of 7-AAD. A region was set around the major populations on a forward/side scatter plot and a gate was set on the 7-AAD negative population. The expression of GFP was analysed in the FL1 channel on a FACS Calibur flow cytometer. (B) The GFP expression in $Sfpi1^{GFP/+}$ and $Sfpi1^{GFP/GFP}$ mice was analysed by flow cytometry as above. Markers show the GFP^{medium} and GFP^{high} regions and numbers denote percentages of positive cells. In the overlay figure, $Sfpi1^{GFP/+}$ samples are shown by a dashed line and $Sfpi1^{GFP/GFP}$ samples by a continuous line. Data is representative of 3–5 mice. (C) RNA was extracted from total bone marrow cells as described in material and methods and the mRNA expression levels of GFP and *Sfpi1* were analysed by qRT-PCR. mRNA levels were normalised to *Hprt*. Error bars show the standard deviation in triplicate samples. A Student's *t*-test was used to test the statistical significance of the mRNA levels in $Sfpi1^{GFP/+}$ and $Sfpi1^{GFP/GFP}$ mice ($p = 0.000004$).

Supplementary data associated with this article can be found, in the online version, at http://dx.doi.org/10.1016/j.leukres.2013.05.019.

3.4. Identification of Sfpi1 copy loss in live leukemic cells

GFP expression in rAML cells was analysed by flow cytometry with 3 cases showing a negative/low expression (52.1f, 61.2f, 51.1c), 3 cases a medium expression (61.3d, 62.2d, 57.3b) and 3 cases a high GFP expression (58.2c, 58.1f, 61.2g) (Fig. 5A).

Knowing that it is possible to distinguish between WT and $Sfpi1^{GFP}$ by PCR with primers specific for exon 5 in *Sfpi1* and the GFP construct, we expected to be able to detect deletions on chromosome 2 [28,30]. Wild type *Sfpi1* gives a product of 680 bp, whereas $Sfpi1^{GFP/+}$ gives a product of 690 bp and 512 bp. For $Sfpi1^{GFP/GFP}$ mice carrying two copies of the GFP construct (*i.e.* 512 bp product), the PCR assay cannot be used to detect deletions of one copy. DNA was

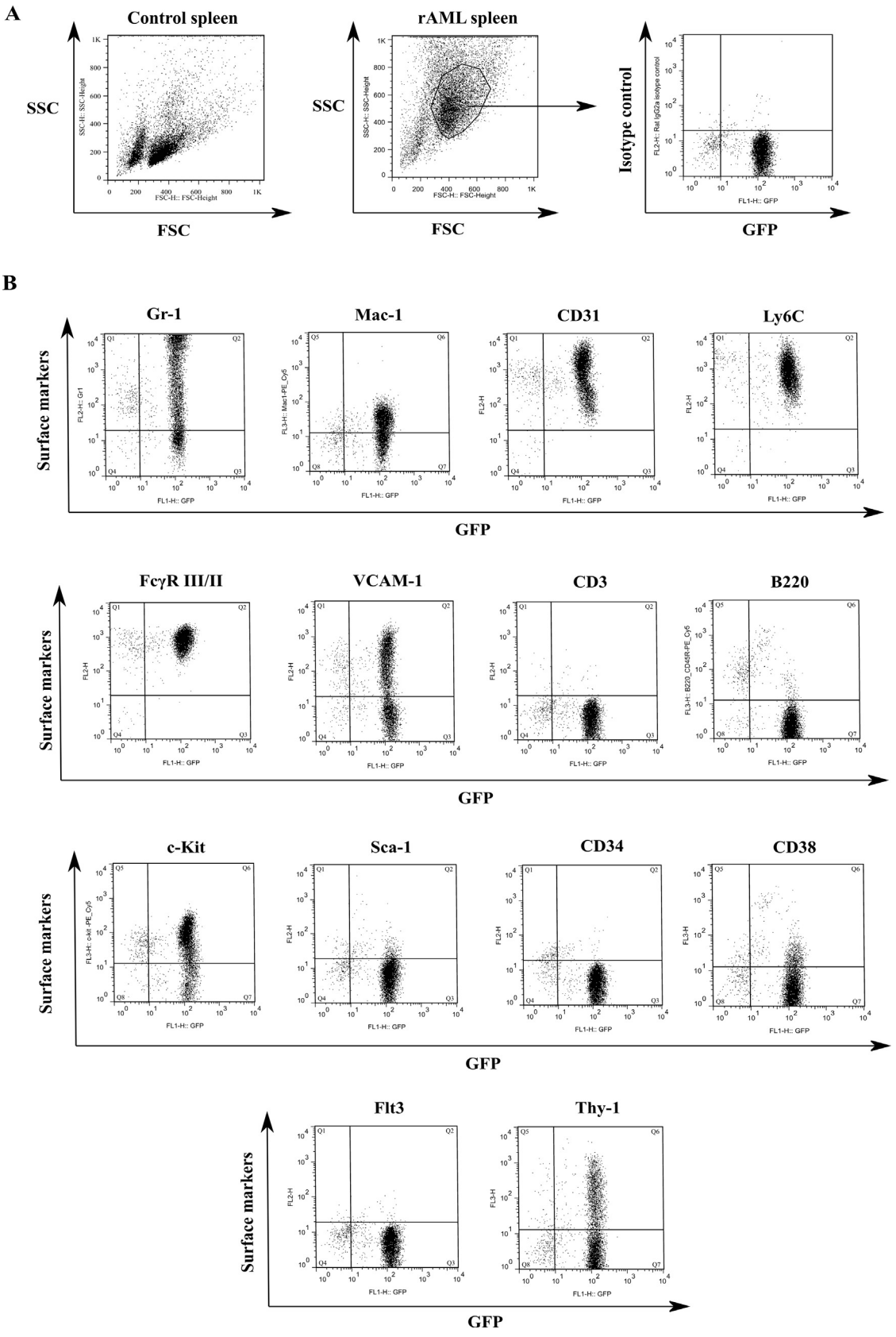

Fig. 4. Immunophenotyping of rAML cases. Single cell suspensions were made of spleen tissue from rAML cases. Cells were stained with fluorescent antibodies specific for various surface markers and analysed by flow cytometry. (A) A gate was drawn around a blast like population with high forward and side scatter, not present in control spleen. Plots were then analysed on a dot plot for GFP expression and a surface marker. (B) Dot plots gated as above for surface markers. Myeloid markers (Gr-1, Mac-1, CD31, Ly6C, FcγR II/II and VCAM-1), T- and B-cell markers (CD3 and B220), myeloid progenitor and haematopoeitic stem cell markers (c-Kit, Sca-1, CD34, CD38, Flt3 and Thy-1).

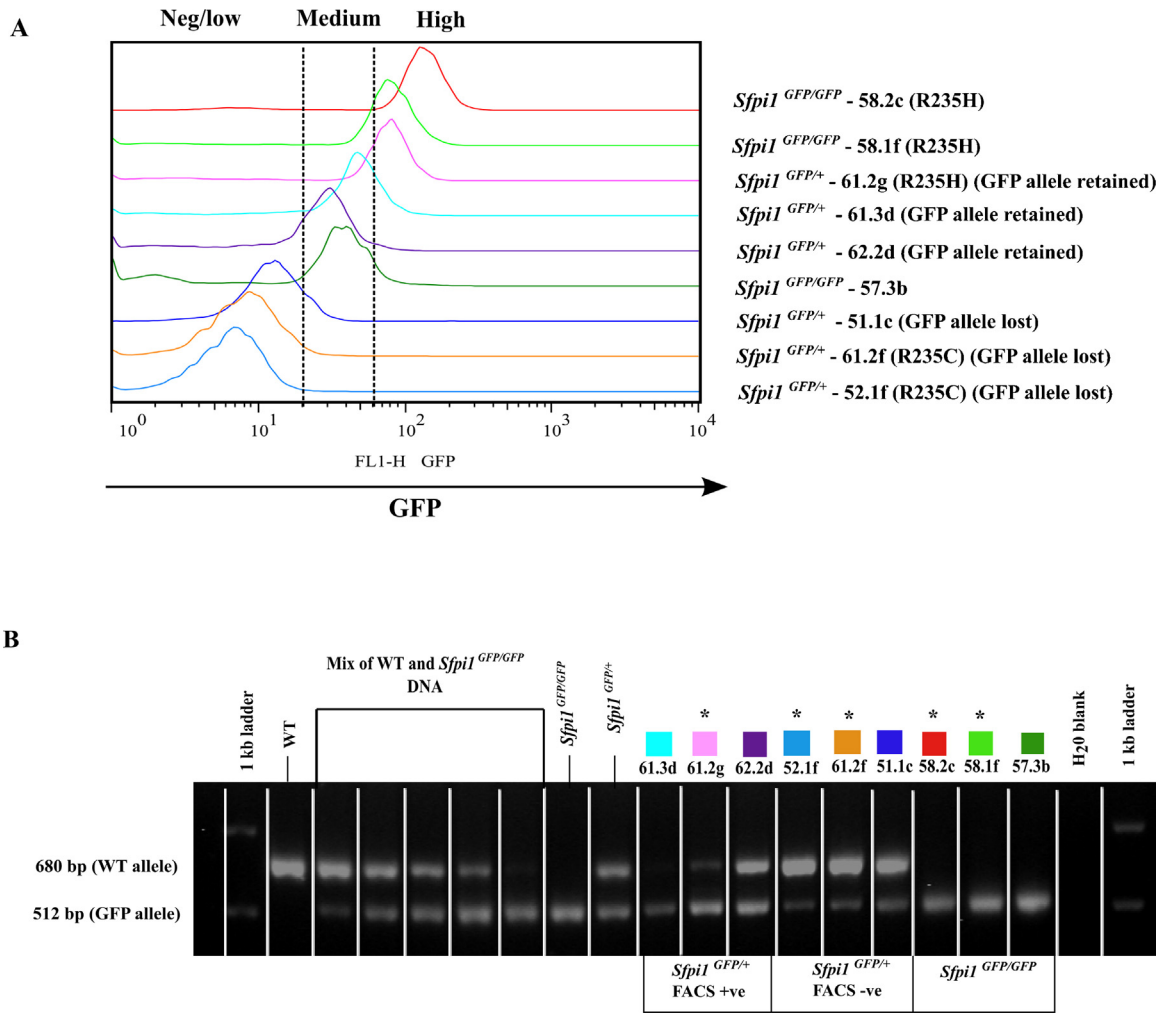

Fig. 5. (A) GFP expression in rAML cases analysed by flow cytometry. The GFP expression in rAML cases displayed in an overlay histogram. On the right hand side, genotype, case name, type of point mutation is labelled. In *Sfpi1*$^{GFP/+}$ mice, whether the GFP allele is lost or retained is noted. (B) PCR genotyping of rAML cases. DNA was extracted from spleen material of control mice (CBA WT, CBA *Sfpi1*$^{GFP+/-}$ and CBA *Sfpi1*$^{GFP+/+}$) and rAML cases. PCR duplex reactions were set up amplifying the region containing the GFP construct and the products were analysed on an agarose gel. WT – 680 bp, *Sfpi1*$^{GFP/GFP}$ – 512 bp, *Sfpi1*$^{GFP/+}$ – 680 bp and 512 bp products respectively. A mix of known concentrations of WT and *Sfpi1*$^{GFP+/+}$ DNA was used to estimate potential contamination of spleen tissue. From left to right (parts WT/*Sfpi1*$^{GFP/GFP}$) 9:1. 7:3, 1:1, 3:7, 1:9. The case names and colour coding is consistent with Fig. 4A. Stars denotes cases with point mutations. FACS^{+}ve: GFP positive, FACS^{-}ve: GFP negative.

extracted from spleen material of CBA/H, *Sfpi1*$^{GFP/+}$ and *Sfpi1*$^{GFP/GFP}$ control mice as well as 9 rAML cases presented (Fig. 5B).

Two of the *Sfpi1*$^{GFP/+}$ mice (61.3d and 61.2g) showed an imbalance in the bands that is similar to that seen in the 1:9 WT/*Sfpi1*$^{GFP/GFP}$ standard. 3 mice (52.1f, 61.2f and 51.1c) showed an imbalance in the bands similar to the 9:1 WT/*Sfpi1*$^{GFP/GFP}$ standard. When the cases were grouped according to whether they showed GFP positivity by flow cytometry analysis, it became clear that the imbalance likely indicated a loss of one allele of *Sfpi1*. The case 61.2g and 61.3d were confirmed by FISH to have lost the WT allele of *Sfpi1* (data not shown). The case that was weakly positive for GFP by flow cytometry analysis, but showed a normal *Sfpi1*$^{GFP/+}$ genotype (62.2d) as assessed by PCR, was confirmed by FISH to be a case where no deletion of *Sfpi1* could be detected. All three cases that were GFP negative by flow cytometry analysis (52.1f, 61.2f and 51.1c) had a majority amplification of the WT allele and were confirmed by FISH to have lost a copy of *Sfpi1*.

The loss of GFP expression assessed by flow cytometry in *Sfpi1*$^{GFP/+}$ mice correlates with the PCR verification of GFP allele loss. *Sfpi1*$^{GFP/+}$ mice without a loss of a *Sfpi1* allele retain a medium GFP expression and the expected *Sfpi1*$^{GFP/+}$ PCR products with two bands. *Sfpi1*$^{GFP/+}$ mice that have lost the non-GFP carrying allele of *Sfpi1* show GFP expression as measured by flow cytometry and the PCR product is that expected from a *Sfpi1*$^{GFP/GFP}$ mouse. FISH was used to confirm all copy loss, which verified results from the flow cytometry and PCR genotyping. In particular, FISH was necessary to confirm *Sfpi1* copy loss in *Sfpi1*$^{GFP/GFP}$ mice where PCR genotyping could not be used (cases 58.2C, 58.1f and 57.3b).

A clear significant correlation between the geometric mean of GFP expression and GFP copy number was obtained in unirradiated BM cells from mice with either 0, 1 or two GFP copies ($p = 0.0324$) and in rAML *Sfpi1*$^{GFP/+}$ cases ($p = 0.008$), thus demonstrating that the expression level of GFP in *Sfpi1*$^{GFP/+}$ rAMLs is depending on the GFP copy being retained or not (Supplementary Fig. 1).

Supplementary data associated with this article can be found, in the online version, at http://dx.doi.org/10.1016/j.leukres.2013.05.019.

Six of the rAMLs analysed in this study have retained a *Sfpi1* GFP allele. Interestingly, 58.2c, 58.1f and 61.2g carry a transition type point mutation G:A in exon 5 of the remaining copy of *Sfpi1* (where the amino-acid R235 is changed to Histidine, codon CGC to CAC) and express higher levels of GFP (geometric mean of 130, 80 and 78 respectively) whereas rAMLS 61.3d, 62.2d and 57.3b (geometric mean of 50, 31 and 37 respectively) have no point mutation in *Sfpi1*.

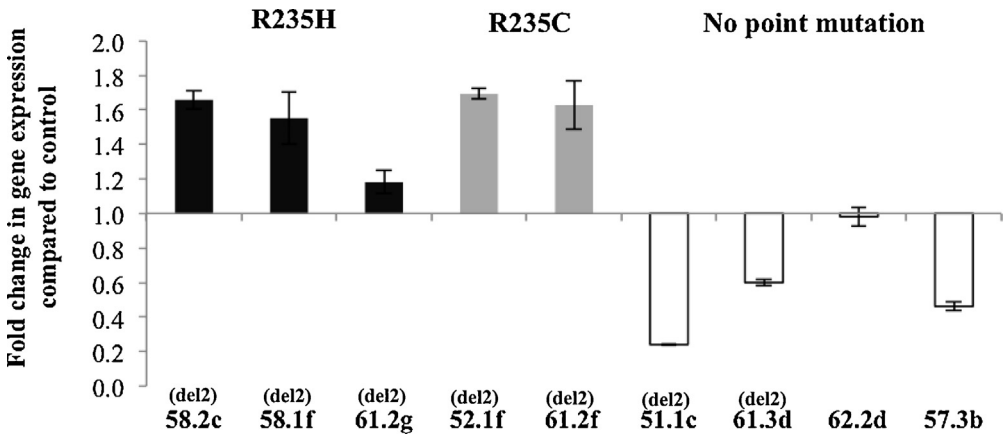

Fig. 6. The expression of *Sfpi1* in rAMl cases. RNA was extracted from rAML spleen cases and the mRNA expression analysed by multiplex-quantitative PCR. Samples were run in triplicate and Ct values were first normalised to the reference gene *Hprt* and converted to transcript quantity using a standard curve. The mRNA expression is shown normalised to the expression of total bone marrow from control mice. The cases are grouped according to the point mutation status. Black: R235H substitution. Grey: R235C substitution. White: Wild type *Sfpi1* allele. The case names are shown below each bar on the chart and del2 indicates cases carrying copy loss of *Sfpi1*. The results show the mean of two independent repeats using two different spleen samples. Error bars represent the standard deviation between independent experiments.

The identification of specific mutations in the DNA binding domain of PU.1 in exon 5 (position R235) are presented in Supplementary Table 1.

3.5. Lower Sfpi1 transcriptional expression in rAMLs without a point mutation in Sfpi1 exon 5

Sfpi1 transcriptional expression in leukaemic infiltrated spleen cells was analysed by qPCR. Results showed that the level of mRNA expression in rAMLs with a point mutation is relatively close to that in the control tissue, mouse bone marrow from non-rAML mice (Fig. 6). This suggests that the level of mutated RNA has not been modified during leukaemogenesis. In contrast, in rAMLs without a *Sfpi1* point mutation (51.1c, 61.3d, 62.2d and 57.3b), leukaemic cells have a lower transcriptional expression of *Sfpi1*.

4. Discussion

IR is a carcinogen that is able to initiate and promote neoplastic development. Experimental investigation of the induction of pre-malignant growths and tumours in laboratory animals exposed to IR has allowed insights into the mechanisms of radiation carcinogenesis, from which better understanding of cancer in humans can be achieved. Technological advances in engineering the mouse genome with chromosome translocations, tissue-specific and/or temporally regulated mutations have provided models which better mimic human cancer [39].

Engineering chromosomal rearrangements in mice using a combination of gene-targeting techniques in mouse embryonic stem cells and the Cre/loxP site-specific recombination system allow the modelling of human diseases that are associated with chromosomal aberrations [40,41]. IR is an efficient clastogen and at sufficiently high doses, chromosome deletions and other chromosome rearrangements are lethal for cells. Nevertheless, it remains uncertain that a chromosome aberration is the key initiation event in radiation carcinogenesis. No specific chromosomal aberrations have been confirmed as the rate-limiting event [42]. This makes it difficult to engineer specific chromosomal rearrangements in mice to mimic radiation-induced cancer. The strongest evidence for a tumour-initiating radiation-induced aberration comes from rAML in CBA mice. Taking advantage of the over-representation of chromosome 2 aberrations in BM cells following IR exposure, more specifically the interstitial deletion (minimal deleted region: D2Mit126 to D2Mit185 representing a chromosome fragment of 21 Mbp), we postulated that the loss of this chromosome fragment carrying a GFP cassette placed next to the *Sfpi1* gene (*sfpi1* exon 5 internal ribosome entry site (IRES) GFP cassette) would be detectable by assessing the decrease (CBA/H $Sfpi1^{GFP/GFP}$) or loss (CBA/H $Sfpi1^{GFP/+}$) of GFP fluorescence [12]. We made use of an engineered mouse model to identify these interstitial deletions *ex vivo* in live leukemic cells by flow-cytometry. Flow cytometry and cell sorting are regularly used to analyse and acquire specific cell populations allowing the study of cells carrying fluorescence emitting reporter genes for specific genes of interest. Significant improvement in the quality of DNA content analysis have been made; high resolution cell cycle profiles and ploidy alterations (DNA-indices as small as 1.09) can be now detected in tumour samples [43]. Flow karyotyping (analysis of chromosomes in suspension by flow-cytometry) can be used to detect chromosomal rearrangements and specific repetitive DNA sequences [44]. Nevertheless, due to technical limitations, chromosomal deletions cannot be detected in individual live cells. Takizawa et al. developed a genetic system for the detection of T(12;15) (Igh-Myc) translocations in plasma cells of a mouse strain in which an enhanced GFP-encoding reporter gene has been targeted to Myc providing a proof of principle that chromosomal aberration can be detected *in vivo* [45]. Here, we have developed a genetic method for the detection of individual chr2del-carrying cells in mice diagnosed with rAML.

We acquired a transgenic mouse model expressing GFP under the *Sfpi1*/PU.1 promoter, and backcrossed it to the CBA/H strain for the use for our purposes [28,30]. In our hands, the GFP expression levels showed a similar profile to the original model with T-cells being negative for GFP expression, B-cells expressing GFP at negative/low levels and myeloid cells such as monocytes and macrophages at high levels (data not shown) [30]. The expression level of GFP protein in the GFP-mouse model was previously shown to be comparable to the level of PU.1 protein and also to have a similar half-life, as assessed by western blotting [28].

We first demonstrated that the introduction of the GFP construct affected neither the genetic susceptibility of mice to radiation-induced AML development nor its time to onset. In these exposed mice diagnosed with rAML, it was possible to look at GFP expression, indicative of *Sfpi1* expression, in individual leukaemic cells in combination with surface marker antibody staining. As in humans, the immunophenotyping of suspected leukaemia cases aids classification of the leukaemia type. In general, individual surface marker expression of the spleen infiltrating blasts showed relatively heterogeneous expression levels between cases, but a

common phenotype was possible to determine (CD31, Ly6c, c-Kit, Mac-1, FcγRIII/II positive, Sca-1, Gr-1, VCAM-1 variable, and CD3, B220, CD34 negative), excluding two cases of biphenotypic leukaemia that were $B220^{+}$ $CD31^{low}$ and $CD38^{high}$. Hirouchi and colleagues recently reported their findings of a common myeloid progenitor – like leukaemic stem cell (LSC) (Lin^{-} $Sca\text{-}1^{-}$ $c\text{-}Kit^{+}$ $CD34^{+}$) in the C3H/He model of rAML [46]. In contrast, in the CBA/H cases presented here, CD34 is generally not expressed. Therefore, a slightly different phenotype may be defined as a LSC for rAML in the CBA/H strain and further work needs to be done to investigate and confirm this.

The reduction of GFP expression in the *Sfpi1*$^{GFP/+}$ mice with a copy loss of *Sfpi1* on the allele carrying the GFP construct was consistent and confirmed by genotyping PCR and FISH. This provides proof of principle that the model can be used to detect partial deletions of chromosome 2.

Furthermore, in the small set of rAMLs studied here, the level of residual GFP expression seems to give a very good indication of the status of the remaining *Sfpi1* allele; remarkably, the detection of the fluorescence level in live leukaemic cells by flow cytometry seems sensitive enough to indicate the presence of a point mutation in the gene, indicating that *Sfpi1*/*PU.1* level is probably tightly regulated in leukaemic cells. The affected amino-acid in rAMLs carrying a point mutation corresponds to R235 which is an integral component of the ETS domain and so DNA binding of the protein [47]. The structure of the wild type and mutant amino acid residues differ significantly and consequently probably modify the protein conformation, influencing the function of the ETS domain for DNA recognition and binding thus impairing PU.1 role as transcription factor. R235H may lead to a totally non-functional protein while PU.1 protein carrying R235C might keep some functionality explaining why it is repressed at the transcriptional level.

In rAMLs where no deletion mutation occurs, the level of PU.1 has to be kept at very low level in cells to avoid differentiation. The mRNA levels in these leukaemic cells suggest that the repression of expression is occurring at the transcriptional levels probably through epigenetic mechanisms.

These results not only provide for a simplification of analysing the deletion status of chromosome 2 in the rAML cases, but also suggest that it might be possible to select and sort by FACS specific subpopulations of cells carrying this deletion at earlier stages in the leukaemic process, long before the presentation of rAML, and to monitor them when transplanted in recipient mice. However, preliminary results (unpublished data) suggests that early time points after exposure to ionising radiation, days or potentially longer, are not suitable since *Sfpi1* is highly expressed due to repopulation of the bone marrow after exposure. Instead we propose a good time point to use the model would be at the time when an expanding clone of cells with interstitial chromosome 2 deletions are present in the bone marrow at 12–15 months after exposure to ionising radiation [13].

Although this model may only imperfectly mimic rAML in humans and the described reporter gene approach requires refinement before it will be possible to investigate the fate of individual haematopoietic progenitors/stem cells that have acquired cancer-associated chromosomal deletion Del2 within their natural microenvironment at an early stage of radiation-induced leukaemia, our findings provide proof of principle that this fluorescent reporter gene system is a viable approach for detecting, enumerating and studying Del2-bearing cells in their normal tissue context. Heterozygous mutations of PU.1 have been found in human AML cases [48]. Furthermore, the gene has also found to be suppressed in some cases of promyelocytic leukaemia, both by the promyelocytic leukaemia-retinoic acid receptor α (PML-RARA) fusion protein and mutations of upstream regulatory elements [49,50]. This study demonstrates that radiation-induced Del2 can be detected in live cancer cells and furthermore R235 type of point mutations can sometimes be inferred. Hence, we provided a useful transgenic mouse experimental system to study radiation-induced AML and mutations of PU.1 in general. To the best of our knowledge, this has not been reported previously.

5. Conclusions

In conclusion, extension of the present reporter gene insertion approach to the pre-malignant state (early after radiation-exposure) should help to gain further understanding of the mechanisms involved in IR-induced leukaemia processes. Following isolation and transplantation, monitoring of these individual pre-leukaemic cells and investigating their fate within their natural microenvironment should prove to be extremely useful in dissecting the steps in tumour initiation, promotion and malignant progression and could lead to new insights into the nature of the molecular mechanisms and identification of the cell of origin in radiation-induced leukaemia, that are relevant for human leukaemia and cancer in general. In the future, this model may also be valuable for preclinical evaluation of therapeutic agents for myeloid leukaemia.

Funding

Financial support was provided by the National Institute for Health Research Centre for Research in Public Health Protection at the Health Protection Agency and by the European Union FP7 DoReMi network of excellence (Grant number 249689). The authors alone are responsible for the content and writing of the paper. This report is work commissioned by the National Institute for Health Research. The views expressed in this publication are those of the authors and not necessary those of the NHS, the National Institute for Health Research or the department of Health.

Conflict of interest statement

The authors report no conflict of interest.

Acknowledgements

The transgenic reporter gene model C57BL/6 *Sfpi1*^{GFP} was generously provided by Prof Steven Nutt from the The Walter and Eliza Hall Institute of Medical Research in Melbourne.

We thank Paul Finnon for immunophenotyping, Francois Paillier for oligonucleotide PCR design, Kevin Whitehill, Donna Lowe, Margaret Coster and Pat Hillier for genotyping and assistance with mouse studies.

Contributions. C-HO designed and performed experiments, analysed the data and wrote and revised the manuscript. RF and NB performed experiments and helped to revise the manuscript. SK performed experiments and analysed data. SDB revised the manuscript. CB conceived of the idea, designed the study and wrote and revised the manuscript.

References

[1] Leone G, Pagano L, Ben-Yehuda D, Voso MT. Therapy-related leukemia and myelodysplasia: susceptibility and incidence. Haematologica 2007;92:1389–98.
[2] Gilbert ES. Ionizing radiation and cancer risks: what have we learned from epidemiology. Int J Radiat Biol 2009;85:467–82.
[3] Sill H, Olipitz W, Zebisch A, Schulz E, Wölfler A. Therapy-related myeloid neoplasms: pathobiology and clinical characteristics. Brit J Pharmacol 2011;162:792–805.
[4] Ron E, Preston DL, Mabuchi K, Thompson DE, Soda M. Cancer incidence in atomic bomb survivors. Part IV: Comparison of cancer incidence and mortality. Radiat Res 1994;137(2 Suppl.):S98–112.

[5] Pierce DA, Shimizu Y, Preston DL, Vaeth M, Mabuchi K. Studies of the mortality of atomic bomb survivors. Report 12. Part I. Cancer: 1950–1990. Radiat Res 1996;146:1–27.
[6] Major IR, Mole RH. Myeloid leukaemia in X-ray irradiated CBA mice. Nature 1978;272:455.
[7] Rithidech K, Bond VP, Cronkite EP, Thompson MH, Bullis JE. Hypermutability of mouse chromosome 2 during the development of X-ray-induced murine myeloid leukemia. Proc Natl Acad Sci USA 1995;92:1152–6.
[8] Azumi J, Sachs L. Chromosome mapping of the genes that control differentiation and malignancy in myeloid leukemic cells. Cancer 1977;74:253–7.
[9] Hayata I, Seki M, Yoshida K, Hirashima K, Sado T, Yamigawa J, et al. Chromosomal aberrations observed in 52 mouse myeloid leukemias. Cancer Research 1983;43:367–73.
[10] Trakhtenbrot L, Krautgamer R, Resnitzky P, Haran-Ghera N. Deletion of chromosome 2 is an early event in the development of radiation-induced myeloid leukemia. Leukemia 1988;2:545–50.
[11] Hirouchi T, Takabatake T, Yoshida K, Nitta Y, Nakamura M, Tanaka S, et al. Upregulation of c-myc gene accompanied by PU.1 deficiency in radiation-induced acute myeloid leukemia in mice. Exp Hematol 2008;36:871–85.
[12] Bouffler SD, Breckon G, Cox R. Chromosomal mechanisms in murine radiation acute myeloid leukaemogenesis. Carcinogenesis 1996;17:655–9.
[13] Bouffler SD, Meijne EIM, Morris DJ, Papworth D. Chromosome 2 hypersensitivity and clonal development in murine radiation acute myeloid leukaemia. Int J Radiat Biol 1997;72:181–9.
[14] Peng Y, Brown N, Finnon R, Warner CL, Liu X, Genik PC, et al. Radiation leukemogenesis in mice: loss of PU.1 on chromosome 2 in CBA and C57BL/6 mice after irradiation with 1 GeV/nucleon 56Fe ions, X rays or γ rays Part I. Experimental observations. Radiat Res 2009;171:474–83.
[15] Cook WD, McCaw BJ, Herring C, John DL, Foote SJ, Nutt SL, et al. PU.1 is a suppressor of myeloid leukemia, inactivated in mice by gene deletion and mutation of its DNA binding domain. Blood 2004;104:3437–44.
[16] Suraweera N, Meijne E, Moody J, Carvajal-Carmona LG, Yoshida K, Pollard P, et al. Mutations of the PU.1 Ets domain are specifically associated with murine radiation-induced, but not human therapy-related, acute myeloid leukaemia. Oncogene 2005;24:3678–83.
[17] Hromas BR, Orazi A, Neiman RS, Maki R, Van Beveran C, Moore J, et al. Hematopoietic lineage- and stage-restricted expression of the ETS oncogene family member PU.1. Blood 1993;82:2998–3004.
[18] Kastner P, Chan S. PU.1: a crucial and versatile player in hematopoiesis and leukemia. Int J Biochem Cell Biol 2008;40:22–7.
[19] DeKoter RP, Singh H. Regulation of B lymphocyte and macrophage development by graded expression of PU.1. Science 2000;288:1439–41.
[20] Dahl R, Walsh JC, Lancki D, Laslo P, Iyer SR, Singh H, et al. Regulation of macrophage and neutrophil cell fates by the PU. 1: C/EBPalpha ratio and granulocyte colony-stimulating factor. Nat Immunol 2003;4:1029–36.
[21] Rosenbauer F, Wagner K, Kutok JL, Iwasaki H, Le Beau MM, Okuno Y, et al. Acute myeloid leukemia induced by graded reduction of a lineage-specific transcription factor, PU. 1. Nat Genet 2004;36:624–30.
[22] Metcalf D, Dakic A, Mifsud S, Di Rago L, Wu L, Nutt S. Inactivation of PU.1 in adult mice leads to the development of myeloid leukemia. Proc Natl Acad Sci USA 2006;103:1486–91.
[23] Finnon R, Brown N, Moody J, Badie C, Olme C-H, Huiskamp R, et al. Flt3-ITD mutations in a mouse model of radiation-induced acute myeloid leukaemia. Leukemia 2012;26:1445–6.
[24] Inomata M, Takahashi S, Harigae H, Kameoka J, Kaku M, Sasaki T. Inverse correlation between Flt3 and PU.1 expression in acute myeloblastic leukemias. Leuk Res 2006;30:659–64.
[25] Brown NL, Finnon R, Bulman R, Finnon P, Moody J, Bouffler SD, et al. Sfpi1/PU.1 mutations in mouse radiation-induced acute myeloid leukaemias affect mRNA and protein abundance and associate with disrupted transcription. Leuk Res 2011;35:126–32.
[26] Alexander BJ, Rasko JE, Morahan G, Cook WD. Gene deletion explains both in vivo and in vitro generated chromosome 2 aberrations associated with murine myeloid leukemia. Leukemia 1995;9:2009–15.
[27] Silver A, Moody J, Dunford R, Clark D, Ganz S, Bulman R, et al. Molecular mapping of chromosome 2 deletions in murine radiation-induced AML localizes a putative tumor suppressor gene to a 1.0 cM region homologous to human chromosome segment 11p11-12. Genes Chromosomes Cancer 1999;24:95.
[28] Nutt SL, Metcalf D, Amico AD, Polli M, Wu L. Dynamic regulation of PU.1 expression in multipotent hematopoietic progenitors. J Exp Med 2005;201:221–31.
[29] Back J, Allman D, Chan S, Kastner P. Visualizing PU.1 activity during hematopoiesis. Exp Hematol 2005;33:395–402.
[30] Dakic A, Metcalf D, Di Rago L, Mifsud S, Wu L, Nutt SL. PU.1 regulates the commitment of adult hematopoietic progenitors and restricts granulopoiesis. J Exp Med 2005;201:1487–502.
[31] Kogan SC, Ward JM, Anver MR, Berman JJ, Brayton C, Cardigg RD, et al. Bethesda proposals for classification of nonlymphoid hematopoietic neoplasms in mice. Blood 2002;100:238–45.
[32] Holmes KL, Otten G, Yokoyama WM. Flow cytometry analysis using the Becton Dickinson FACS calibur. Curr Protoc Immunol 2001, 5.4.1–22.
[33] Clark D, Meijne E, Bouffler S, Huiskamp R, Skidmore CJ, Cox R, et al. Microsatellite analysis of recurrent chromosome 2 deletions in acute myeloid leukaemia induced by radiation in FI hybrid mice. Genes Chromosomes Cancer 1996;16:238–46.
[34] Kabacik S, Ortega-Molina A, Efeyan A, Finnon P, Bouffler S, Serrano M, et al. A minimally invasive assay for individual assessment of the ATM/CHEK2/p53 pathway activity. Cell Cycle 2011;10:1152–61.
[35] Kabacik S, Mackay A, Tamber N, Manning G, Finnon P, Paillier F, et al. Gene expression following ionising radiation: identification of biomarkers for dose estimation and prediction of individual response. Int J Radiat Biol 2010;87:115–29.
[36] Weil MM, Bedford JS, Bielefeldt-Ohmann H, Ray FA, Genik PC, Ehrhart EJ, et al. Incidence of acute myeloid leukemia and hepatocellular carcinoma in mice irradiated with 1 GeV/nucleon 56Fe ions. Radiat Res 2009;172:213–9.
[37] Major IR. Induction of myeloid leukaemia by whole-body single exposure of CBA male mice to X-rays. Brit J Cancer 1979;40:903–13.
[38] Iwasaki H, Akashi K. Myeloid lineage commitment from the hematopoietic stem cell. Immunity 2007;26:726–40.
[39] Jackson-Grusby L. Modeling cancer in mice. Oncogene 2002;21:5504–14.
[40] Yu Y, Bradley A. Engineering chromosomal rearrangements in mice. Nat Rev Genet 2001;2:780–90.
[41] Tuveson DA, Jacks T. Technologically advanced cancer modeling in mice. Curr Opin Genet Dev 2002;12:105–10.
[42] Goodhead DT, Fifth Warren K. Sinclair keynote address: issues in quantifying the effects of low-level radiation. Health Phys 2008;97:394–406.
[43] Heinlein C, Deppert W, Braithwaite A, Speidel D. A rapid and optimization-free procedure allows the in vivo detection of subtle cell cycle and ploidy alterations in tissues by flow cytometry. Cell Cycle 2010;9:3584–90.
[44] Brind'Amour J, Lansdorp P. Analysis of repetitive DNA in chromosomes by flow cytometry. Nat Methods 2011;8:6–10.
[45] Takizawa M, Kim JS, Tessarollo L, et al. Genetic reporter system for oncogenic Igh-Myc translocations in mice. Oncogene 2010;29:4113–20.
[46] Hirouchi T, Akabane M, Tanaka S, Braga-Tanaka III I, Todate A, Ichinohe K, et al. Cell surface marker phenotypes and gene expression profiles of murine radiation-induced acute myeloid leukemia stem cells are similar to those of common myeloid progenitors. Radiat Res 2011;176:311–22.
[47] Poon GMK, Macgregor Jr RB. Base coupling in sequence-specific site recognition by the ETS domain of murine PU.1. J Mol Biol 2003;328:805–19.
[48] Mueller BU, Pabst T, Osato M, Asou M, Johansen LM, Minden MD, et al. Heterozygous PU.1 mutations are associated with acute myeloid leukemia. Blood 2002;100:998–1007.
[49] Mueller BU, Pabst T, Fos J, Petkovic V, Fey MF, Asou M, et al. ATRA resolves the differentiation block in t (15;17) acute myeloid leukemia by restoring PU.1 expression. Blood 2006;107:3330–8.
[50] Bonadies N, Neururer C, Steege A, Vallabhapurapu S, Pabst T, Mueller BU. PU.1 is regulated by NF-kappaB through a novel binding site in a 17 kb upstream enhancer element. Oncogene 2010;29:1062–72.